Specific Absorption Rate (SAR) Analysis Using Finite Difference Time Domain Computation for RF Transmitter Circuit Employed in Biotronik Lexos "T" Implantable Cardiac Defibrillators

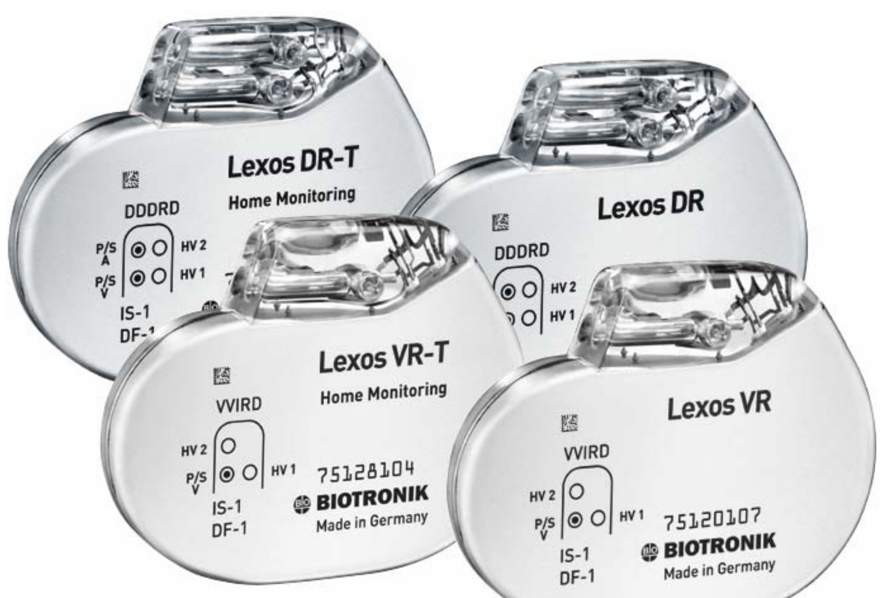

October 7, 2003

Introduction

Biotronik has developed an RF communications system for use in implantable pacemakers and Implantable Cardiac Defibrillators (ICDs) allowing for patient data regarding cardiac condition to be transmitted wirelessly to the physician for evaluation. The amount of irradiated power transmitted through the human body using this technology can be defined by a measure termed the Specific Absorption Rate (SAR). Values of SAR that can be safely used in these applications have been defined by ANSI/IEEE and are part of the FCC guidelines for medical implant communications.

Certification of medical-implant transmitters under the FCC Part 95 Medical Implant Communication Service (MICS) requires a measurement or Finite Difference Time Domain (FDTD) analysis of the SAR associated with the presence of a non-ionizing, radio frequency (RF) transmitter. This report details the SAR analysis of the unidirectional RF transmitter found in Biotronik's Lexos "T" family of ICDs.

Biotronik performed this analysis on a previous implantable devices designated as the BA03 DDDR pacemaker and the Belos "T" family of ICDs. The analyses for these devices were performed using a FDTD tool and the equipment authorization for these devices are listed under FCC identifiers PG6BA0T and PG6BELOS-T. The RF circuit utilized in Lexos ICD is directly comparable to the BA03 pacemaker and Belos "T".

Summary

Using a commercially available FDTD program (XFDTD, Remcom Inc.), the computed SAR values determined by this analysis are:

Maximum SAR	277 mW/kg
Maximum 1 gm average SAR	2.9 mW/kg
Maximum 10 gm average SAR	951 µW/kg
Average SAR	99 µW/kg

The ANSI C95-1-1992 limit is 1.6 W/kg. The computed value in this study of the maximum SAR in a 1 gram average is 2.9 mW/kg. The margin between the maximum attained SAR and the ANSI/IEEE specification limit is 27.4 dB (only 0.18 % of the specification limit). An uncertainty analysis (worst case) of this computation (detailed in Appendix A) subtracts 3.34 dB from this margin to yield a 1 gram average that is 24 dB below the 1.6 W/kg limit.

These FDTD results prove that the Biotronik RF transmitter circuitry can safely be used in its intended application with respect to the energy emitted during communication.

Method of Analysis

The computational tool used for this FDTD analysis was XFDTD. The 3D import tool (available from Remcom with version 5.3) with was used to convert a 3D solid model of the ICD to a rectangular-grid FDTD computational space. A uniform cell size of 1/2 mm was used. This allowed modeling of the antenna in the header. As the cell size is very small, it is not practical to include a model of the upper torso with the ICD. Previous experience using FDTD modeling methods showed that the region of maximum SAR is concentrated very near the antenna. Thus the model used in this study was restricted to at least 2 cm of tissue around the ICD. This limited the computational space to 8 million cells. The figure below shows a 3D view of the computational space. The computational space used was 12 x 12 x 7 cm^3 or approximately 1000 cm^3. This computational volume allowed 1 gram and 10 gram average SAR results.

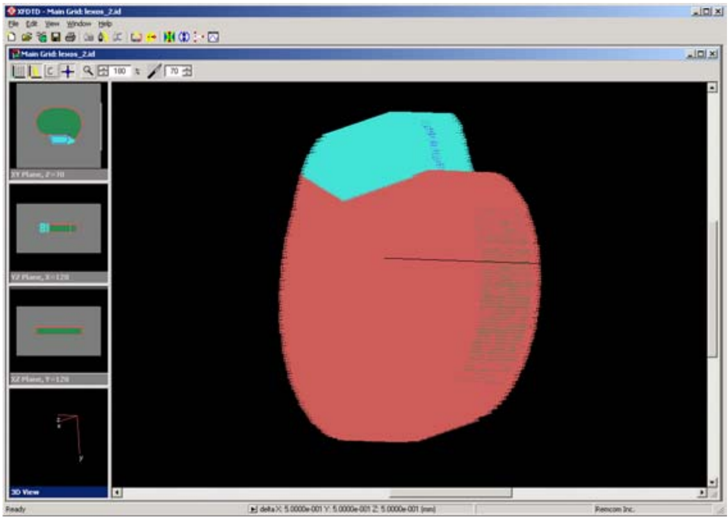

The use of a small cell size allowed all elements of the structure to be realized with "non-thin" FDTD models. The source power and impedance used to drive the antenna were determined by the measurements outlined in Appendix A. The material electrical properties were obtained from either tabulated data or direct measurement using a dielectric probe. Specifically, the relative dielectric constant of the header epoxy (cyan) is ~3 and the conductivity is ~ 0.001 S/m. The electrical properties of the biological material were $\varepsilon_r = 54$ and $\sigma = 0.66$ S/m. The case and antenna are titanium (salmon). The space inside the case and the epoxy header were not included in the computation of the SAR, hence the results indicated are due to absorption in the tissue.

The analysis was performed at 403 MHz. XFDTD provides an application to compute the SAR at a single frequency. In the MICS band, the electrical properties of biological tissue are described by a dipolar mechanism. The dipolar region is characterized by slowly changing permittivity and conductivity, with many tissue types exhibiting a Cole-Cole behavior. Thus, it is reasonable to expect similar SAR results over the entire MICS band.

The photo below shows the SAR statistics from this computation. These statistics were used to summarize the results stated above.

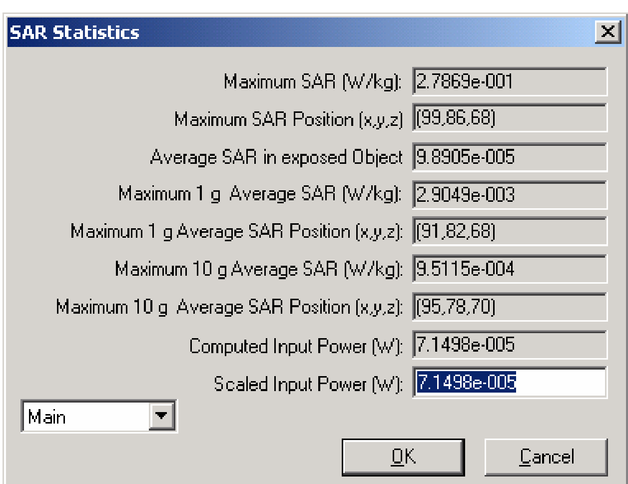

SAR Statistics

Maximum SAR (W/kg):	2.7869e-001
Maximum SAR Position (x,y,z)	(99,86,68)
Average SAR in exposed Object	9.8905e-005
Maximum 1 g Average SAR (W/kg):	2.9049e-003
Maximum 1 g Average SAR Position (x,y,z):	(91,82,68)
Maximum 10 g Average SAR (W/kg):	9.5115e-004
Maximum 10 g Average SAR Position (x,y,z):	(95,78,70)
Computed Input Power (W):	7.1498e-005
Scaled Input Power (W):	7.1498e-005

Main

OK Cancel

A photo of the header of the ICD "T" family is shown below. In this photo, the loop antenna is easily identifiable embedded in the header of the device (around the perimeter).

Equipment and tools used for the analysis:

Hardware

Dell dual processor Windows 2000 Workstation, 1 Gb RAM 3 drive SCSI RAID
Hewlett-Packard 8591 Spectrum Analyzer
Hewlett Packard 8753E Vector Network Analyzer
Agilent 85070C Dielectric Probe

Software

XFDTD (Remcom) 5.3.0.2 Bio-Pro, Calc FDTD 5.3, Remesher 5.3, HIFI Body model

Conclusions:

As shown from this Finite Difference Time Domain analysis, the RF transmitter used by Biotronik in the Lexos ICD meet the Specific Absorption Rate (SAR) standard set by ANSI/IEEE and incorporated into the FCC guidelines for medical implantable communications devices. The specific results reveal that the computed maximum SAR value for this RF circuit with measurement uncertainty has a margin of 24 dB to the specification limit.

Appendix A

Below are the details of the methods used to obtain the results stated in this SAR calculation. This section describes the methods used to derive electrical properties of the tissue, an uncertainty analysis to modify the SAR 1 and 10 gram maximums due to instrument uncertainties, locations of the antenna feed point, the details of the locations and values of the 1 and 10 gram SAR maximums, the measurement techniques used to obtain the output power and source impedance, and the location of the implant in a human torso.

Tissue parameters used in this analysis

The dielectric fluid used in the torso model was obtained from the paper "Simulated Biological Materials for Electromagnetic Radiation Absorption Studies" G. Hartsgrove et.al. This paper is referenced by the FCC for use in the torso model for MICS band emissions tests (95.639). The conductivity and permittivity specified in this report are typical for the implant region where a combination of muscle, fat, and lung tissue is likely to be found. Electromagnetic values for these tissue types are documented by C. Gabriel et.al., and can be found on-line at http://www.brooks.af.mil/AFRL/HED/hedr/reports/dielectric/cover.html.

Details of the uncertainty analysis used in this calculation

The uncertainty analysis described below considers the error in the vector reflectometer used to measure the source impedance of the RF transmitter in the implant, the errors associated with the spectrum analyzer used to measure the output power of the implant, and the uncertainty in the spectrum analyzer measurement due to the non-ideal return loss of the spectrum analyzer and the coax connection. Each of these 3 error types will be summarized in a table and the worst-case sum of these effects will be used to modify the SAR calculation. Of interest here is the possible increase in SAR (reduction of spec margin).

Reflectometer error

An Agilent 8753ES vector network analyzer was used to measure the output impedance from the implant RF transmitter. The 8753ES was calibrated for a 1-port S11 measurement using an open, short and load. (NIST traceable Agilent 85033D 3.5 mm Calibration Kit)
Typical measurement error associated with a reflection calibration is found in the specifications for the 8753ES, and at 400 MHz for $\Gamma = 0.374 + j0.245$, the uncertainty for $|\rho|$ is ± 0.01; Arg(Γ) is $\pm 1°$.

Spectrum analyzer amplitude error

The amplitude error associated with an Agilent 8595E for the test conditions (-10 dBm reference level, 1 KHz resolution BW, 1 KHz video BW, 10 dB attenuation, DC coupling) are summarized in the table below:

Amplitude accuracy $\pm(.3\,dB + .01 \cdot (-1.64 - -20))$	$\pm 0.484 dB$
Resolution BW switching uncertainty	$\pm 0.6 dB$
Attenuator uncertainty $\pm .8 dB\ per 10\, dB$	$\pm 1.6 dB$

Return loss error

Figure 1 shows the signal flow graph for the transmitter impedance measurement.

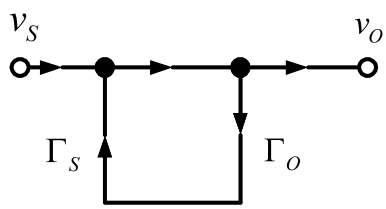

Figure 1 Signal flow graph of the transmitter connected to the spectrum analyzer

The transfer function from source to output is

$$\frac{v_S}{v_O}=\frac{1}{1-\Gamma_S\cdot\Gamma_O}$$

The uncertainty associated with this transfer function ("Microwave Theory and Applications", Stephen Adam, Prentice-Hall pg 233) is,

$$(1\pm|\Gamma_S|\cdot|\Gamma_O|)^2 .$$

For the nominal values of $\Gamma = 0.374 + j0.245$ and $\Gamma_0 = 0.1304$ (the 8595E has a VSWR of 1.3:1) the uncertainty is $(1\pm 0.1304\cdot 0.447)^2$, or –0.522 to +0.492 dB.

Figure 2 shows the equivalent circuit associated with the method used to derive the source impedance.

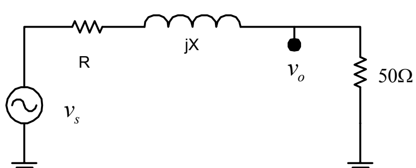

Figure 2 Determination of source voltage

Here the output load is a nominal 50Ω, (within a VSWR of 1.3:1) and the nominal source impedance is 88.4 Ω in series with 21.4 nH of inductance. The data taken from the 8753ES is shown in Figure 3.

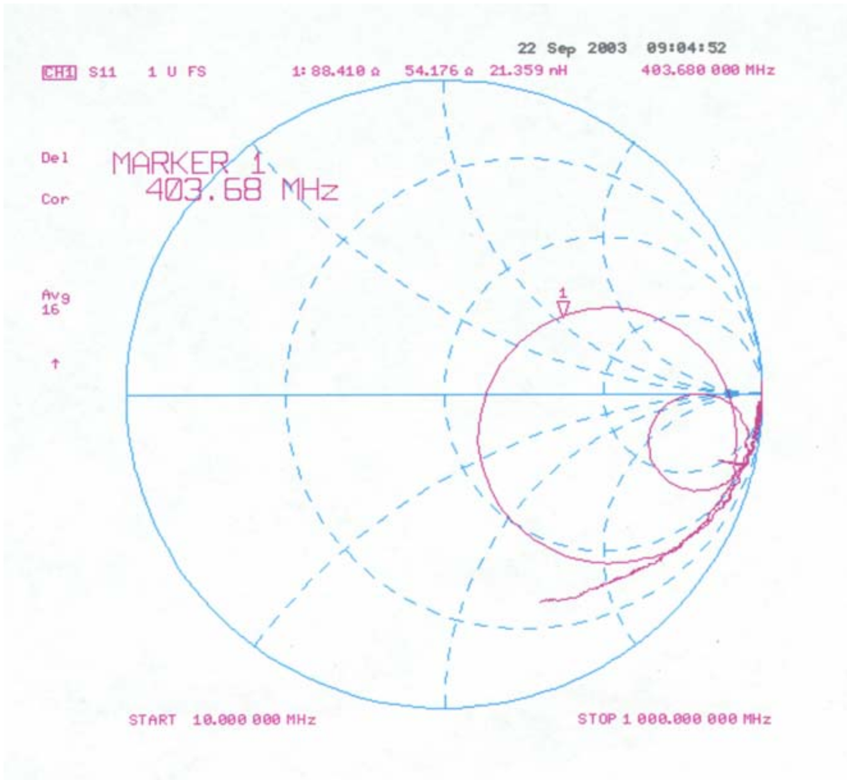

Figure 3 Transmitter reflection measurement

Referring to Figure 2, the output voltage v_S, will be maximized when the expression for v_S is maximized,

$$|v_S| = \sqrt{\frac{P_O}{50} \cdot \left((50 + R_S)^2 + X_S^2\right)} \qquad (1)$$

For the nominal values of the source impedance and measured output power (-1.64 dBm), the nominal magnitude of the transmitter voltage is 778 mV_p.

To complete the uncertainty analysis we will apply the uncertainty of the network analyzer and the amplitude accuracy of the spectrum analyzer to the above equation. The uncertainty due to the finite return loss of the spectrum analyzer will be attributed to the power P_O of the spectrum analyzer.
The values of R_S and X_S are maximized when the uncertainty in $|\rho|$ is +.01 and Arg(Γ) is $-1°$. For this case R_S = 90.7 Ω and X_S = 56.0 Ω.
For maximizing P_O, we have,

P_O = -1.64 dBm + 0.484 dB +0.6 dB + 1.6 dB + 0.492 dB = 1.54 dBm or 1.42 mW

Substituting all of the parameter changes to compute the worst-case uncertainty,

$$|v_S| = \sqrt{\frac{1.42mW}{50} \cdot \left((50 + 90.7)^2 + 56.0^2\right)} = 808 \text{ mV}_{RMS} = 1.14 \text{ mV}_p$$

This is an increase of $20 \cdot \log_{10}\left(\frac{1.14}{0.778}\right)$ or 3.34 dB. As the SAR is dependent on the square of the electric field component, and the dielectrics modeled are all isotropic and linear, the increase in the SAR is 3.34 dB.

Details of the antenna feed modeling

Figure 4 shows the sources summary from XFDTD.

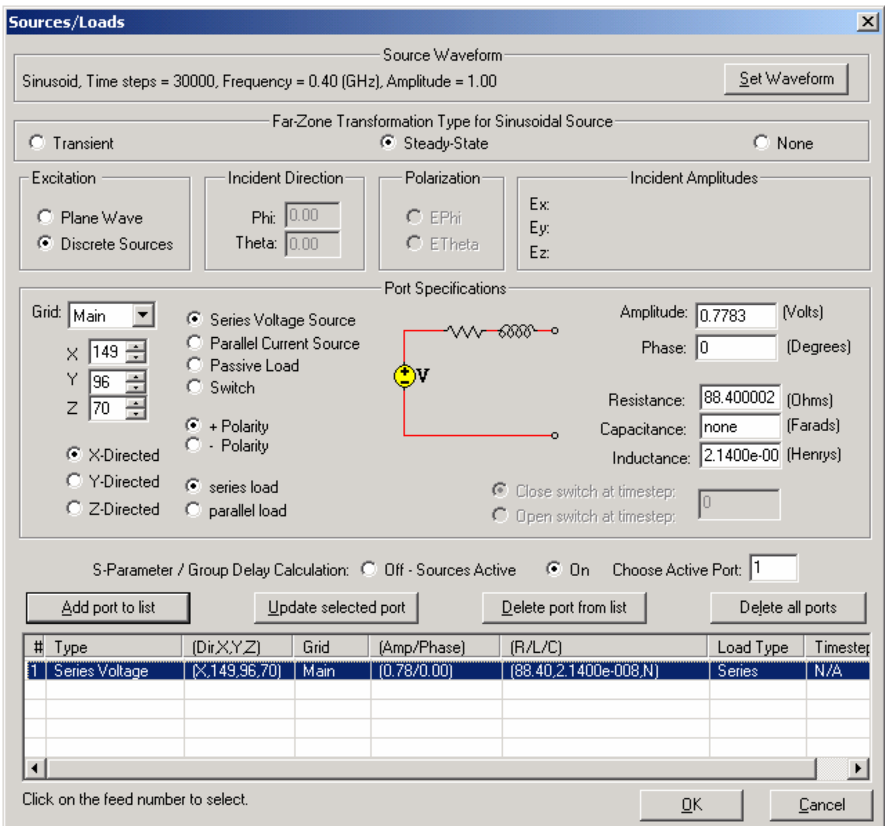

Figure 4 Details of the source used in the SAR analysis

This shows that a 0.778 mV_p source was placed at location (149,96,70) (x,y,z). The source impedance was a series RL network with the same element values derived from the reflection measurement shown in Figure 3. Figure 5 shows the source located in the z=70 plane of the geometry model.

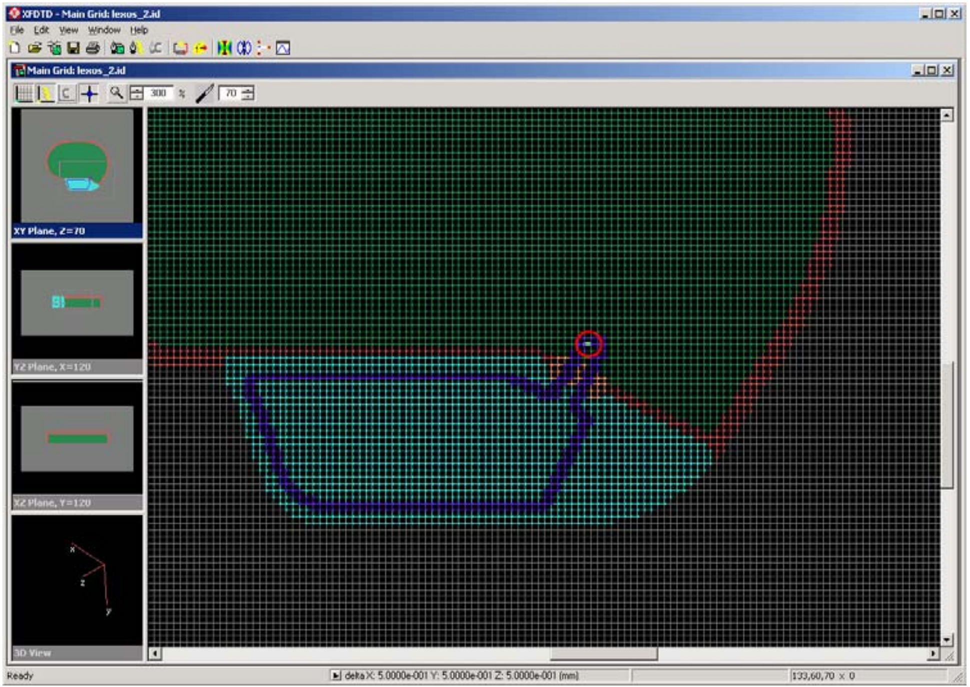

Figure 5 Location of source in model geometry

Loop antenna details and 3D renderings of the structure used to compute the SAR.

The details of the antenna are shown in the following figures. Figure 6 shows a 3D solid model of the Lexos ICD with the tissue dielectric removed in this photo for clarity.

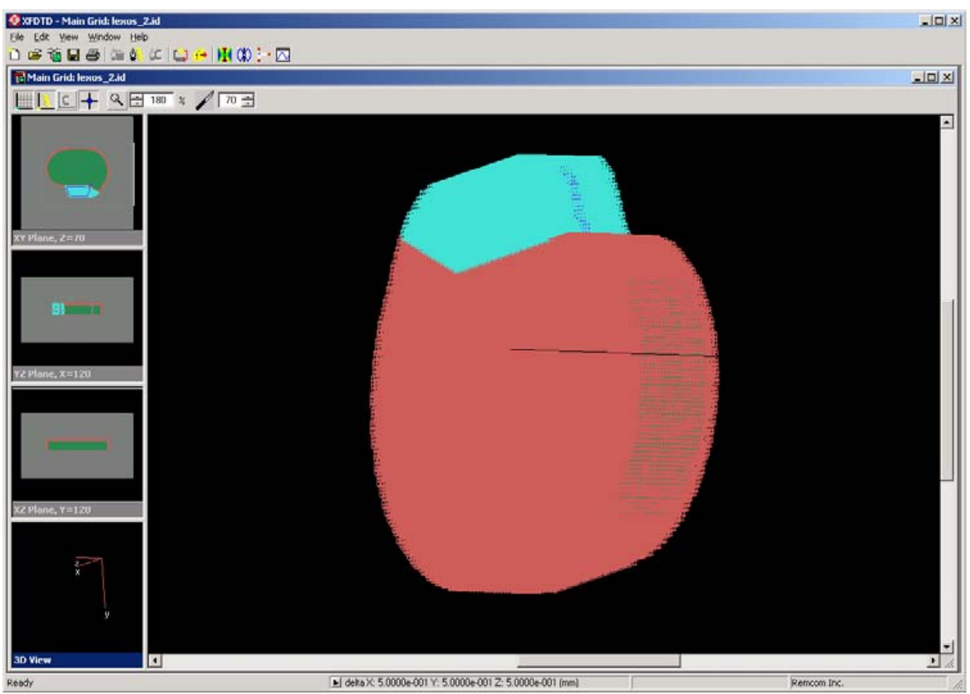

Figure 6 3D solid model of Lexos ICD (tissue removed for clarity)

In Figure 6 the titanium housing is shown in salmon, and the epoxy header containing the loop antenna is shown in cyan. In Figure 7, the tissue and the epoxy header are removed to show the loop antenna (blue) within a 3D rendering. The antenna feedthrough (tan) can be also be seen in Figure 7.

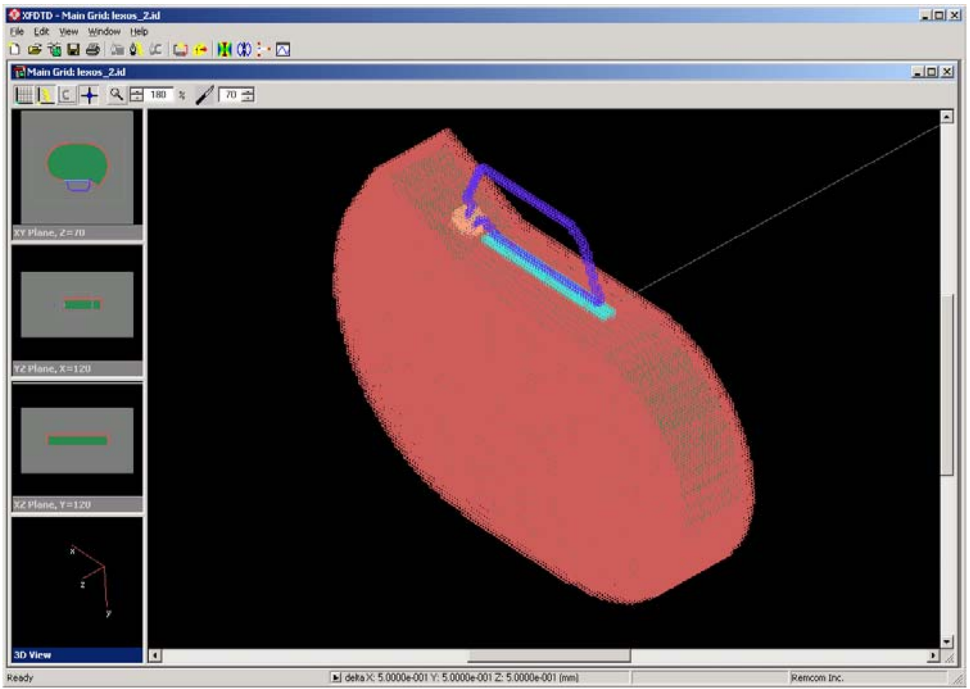

Figure 7 3D model of Lexos ICD showing loop antenna (header and tissue removed for clarity)

Details of how the spectrum analyzer and network analyzer were used to measure output voltage and output impedance

The Lexos ICD was programmed to transmit a CW signal. The 8753ES vector network analyzer was calibrated through a 50Ω test coax that was de-embedded along with the network analyzer calibration. A SMA connector was soldered to the antenna pads on the hybrid, and the length of the SMA connector was removed by electrically extending the reference plane of the network analyzer. For the 0.3” length of this SMA launch, it is acceptable to treat the launch as a section of lossless coax at 400 MHz. A short placed at the antenna pads allowed the new reference plane to be established and showed that the assumption of a lossless coax model of the connector was accurate. As the Lexos ICD transmitter was operational, the 8753ES test port power was varied from –30 dBm to –10 dBm and the locus of the reflection coefficient was noted on the Smith chart. The locus varied very little over this range, indicating that the output impedance of the ICD transmitter was relatively insensitive to loading in a 50Ω environment. The data was taken with a test port power of –30 dBm and the transmitter was active during this test. This details the method used to obtain the output impedance.

Figure 2 shows the equivalent circuit used to determine the transmitter source voltage. The Lexos transmitter was connected to the 8595E spectrum analyzer through a SMA coupler (negligible loss at 400 MHz). The output power was measured and equation (1) was used to derive the magnitude of this source. Impedance in a 50Ω environment was thus preserved in the determination of the source impedance and also in the measurement of the output power.

Details of maximum 1 gram and 10 gram SAR indicating location

Figures 8 and 9 show the un-averaged SAR 1/2 mm above and below the metal case. In these photos, the epoxy header can be seen, as it is thicker than the metal case.

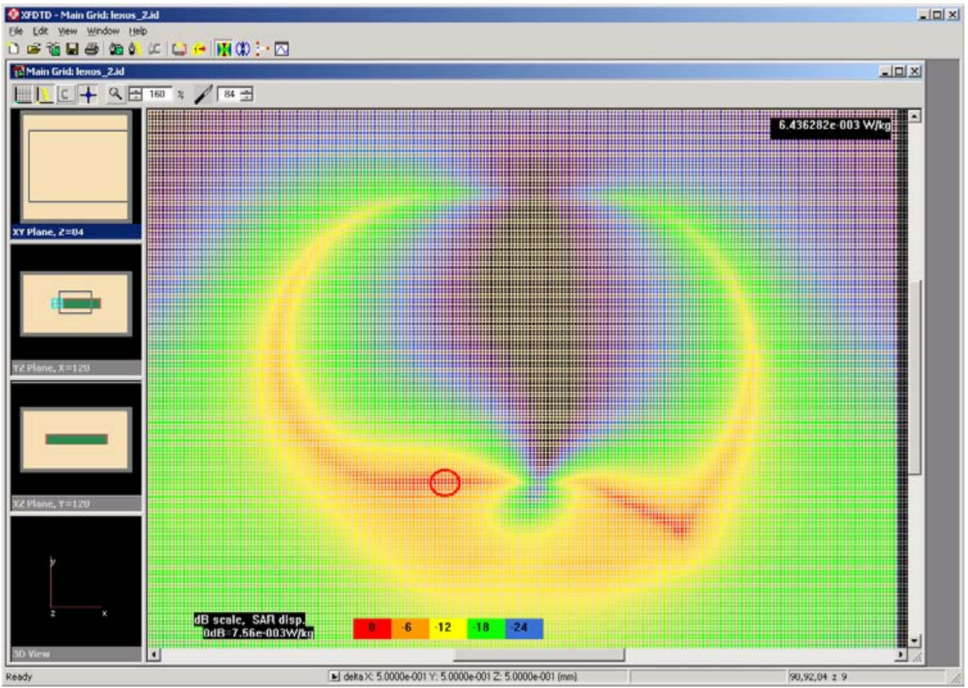

Figure 8 Un-averaged SAR at a location 1/2 mm above the metal case The red circle indicates that the maximum SAR is 6.44 mW/kg.

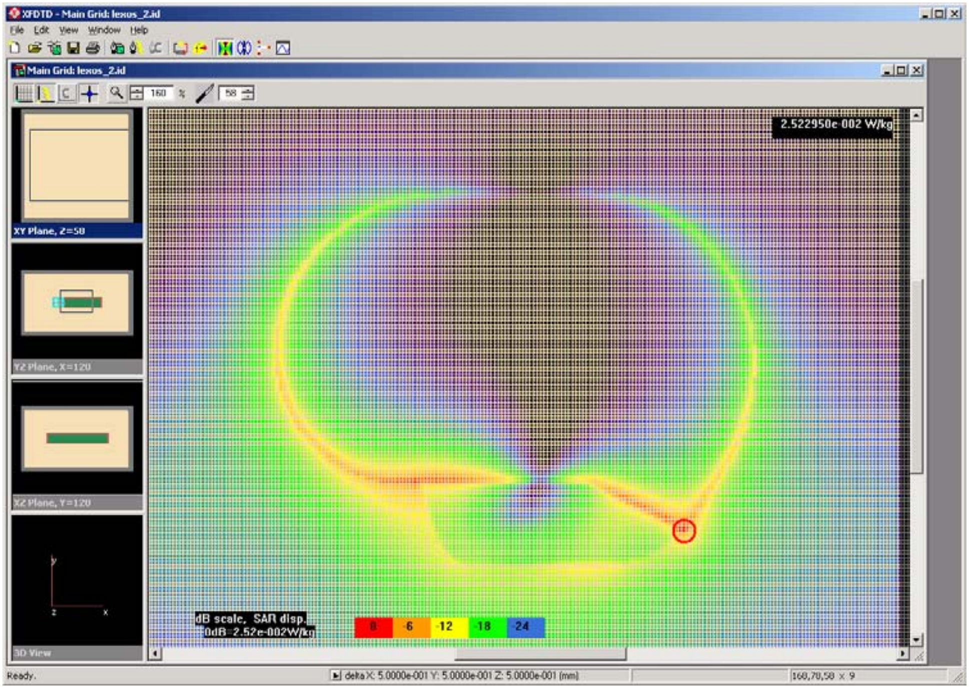

Figure 9 Un-averaged SAR at a location 1/2 mm below the metal case. The red circle indicates that the maximum SAR is 25.2 mW/kg.

For these 2 cases, the un-averaged SAR is less than 30 mW/kg.

Figure 10 shows the 1 gram averaged maximum SAR. This maximum is located just to the left of the header.

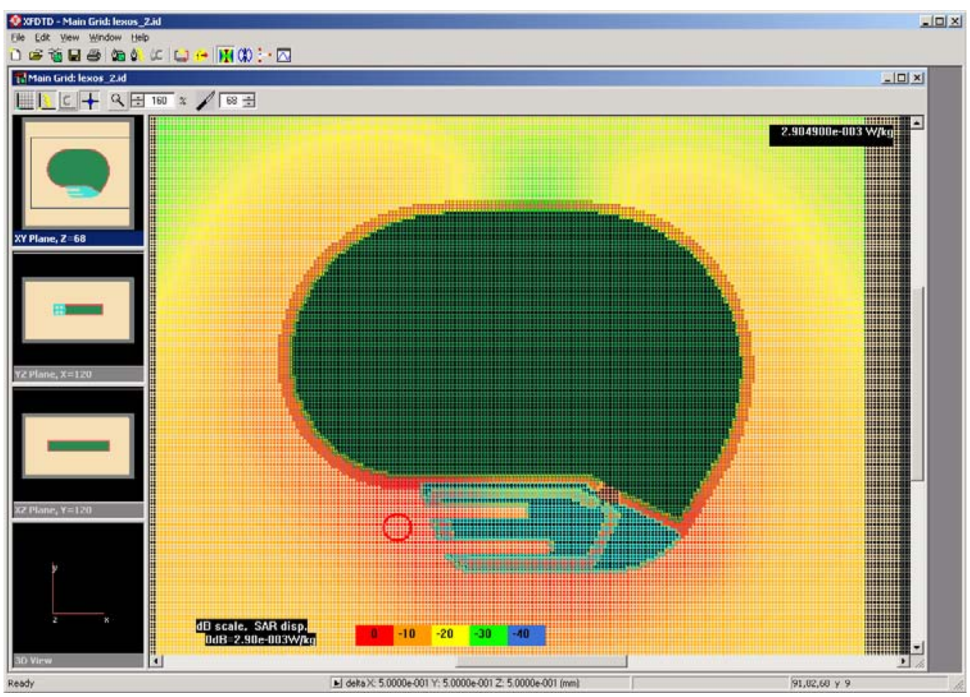

Figure 10 1 gram average maximum SAR depicted by the red circle. The maximum 1 gram average is 2.9 mW/kg.

Figure 11 shows the maximum 10 gram averaged SAR. This maximum is also located just to the left of the header.

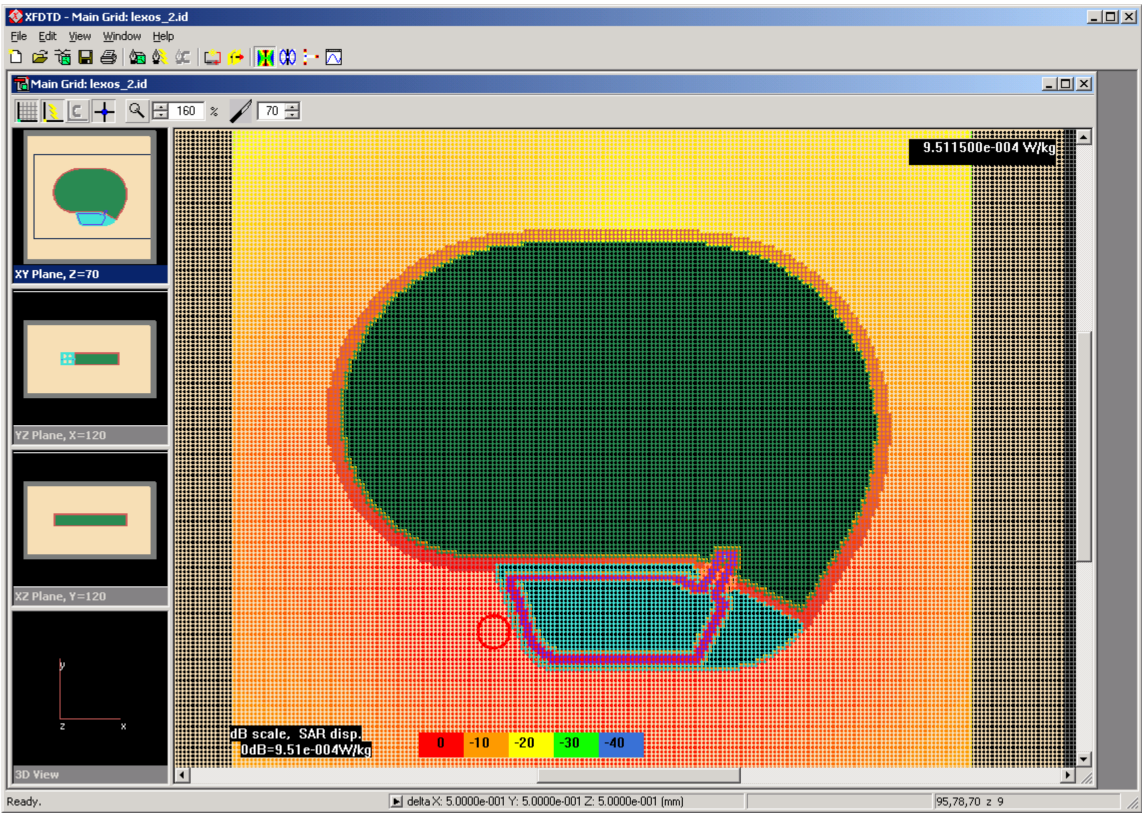

Figure 11 10 gram average maximum SAR depicted by the red circle. The maximum 10 gram average is 951 µW/kg.

Figures 10 and 11 show a maximum 1 gram and 10 gram average of 2.9 mW/kg and 951 µW/kg respectively.

Figures 12 through 15 show the 1 gram averages at locations 0.5 cm, 1 cm, and 1.5 cm above and below the Lexos ICD.

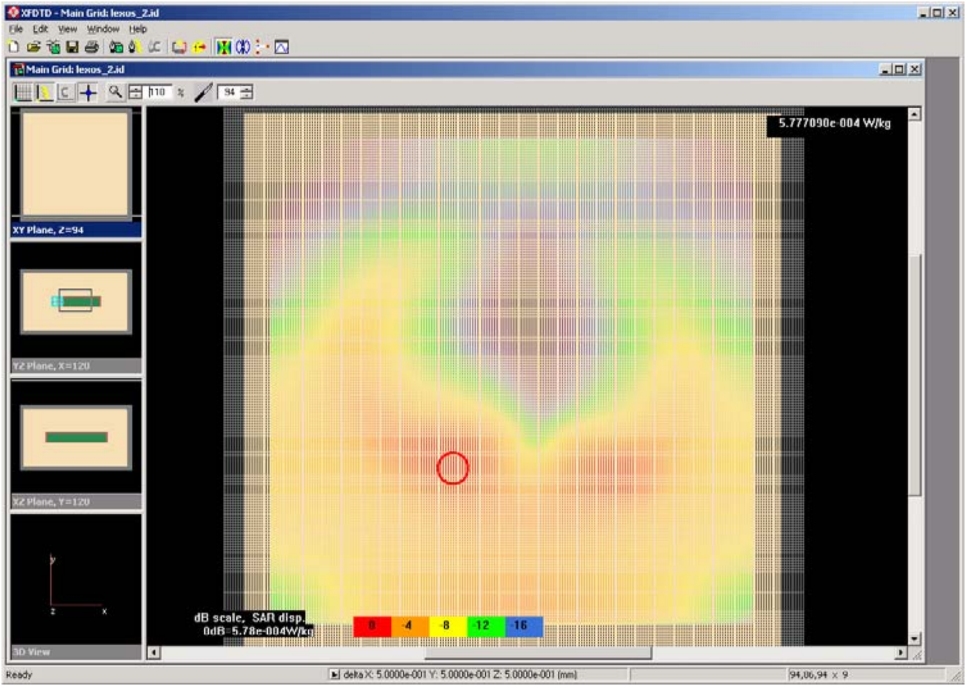

Figure 12 1 gram SAR average 5 mm above Lexos. A maximum SAR of 578 µW/kg is indicated.

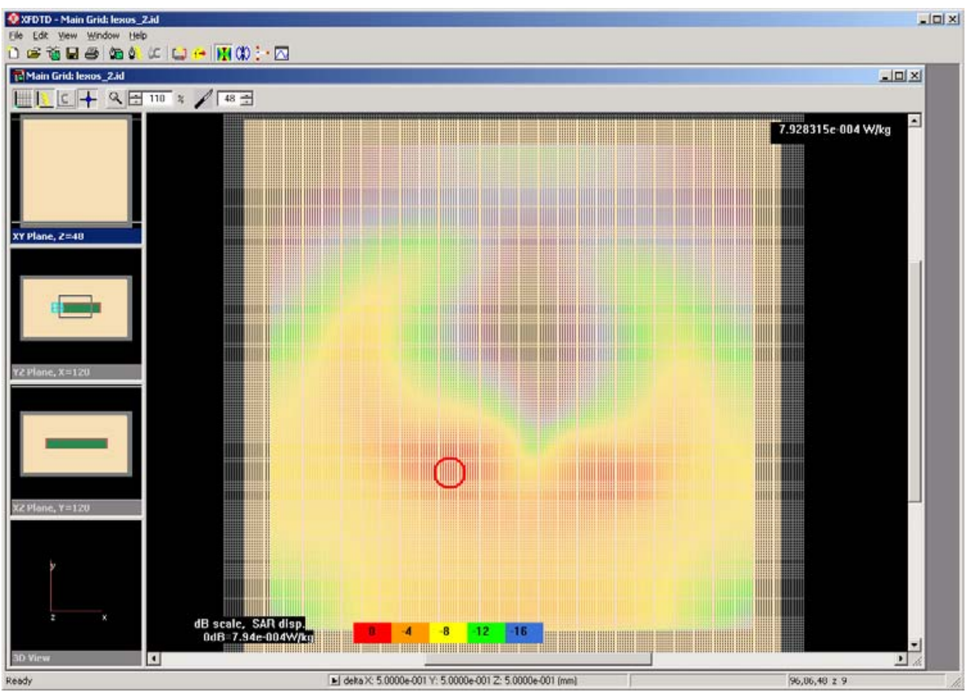

Figure 13 1 gram SAR average 5 mm below Lexos. A maximum SAR of 793 µW/kg is indicated.

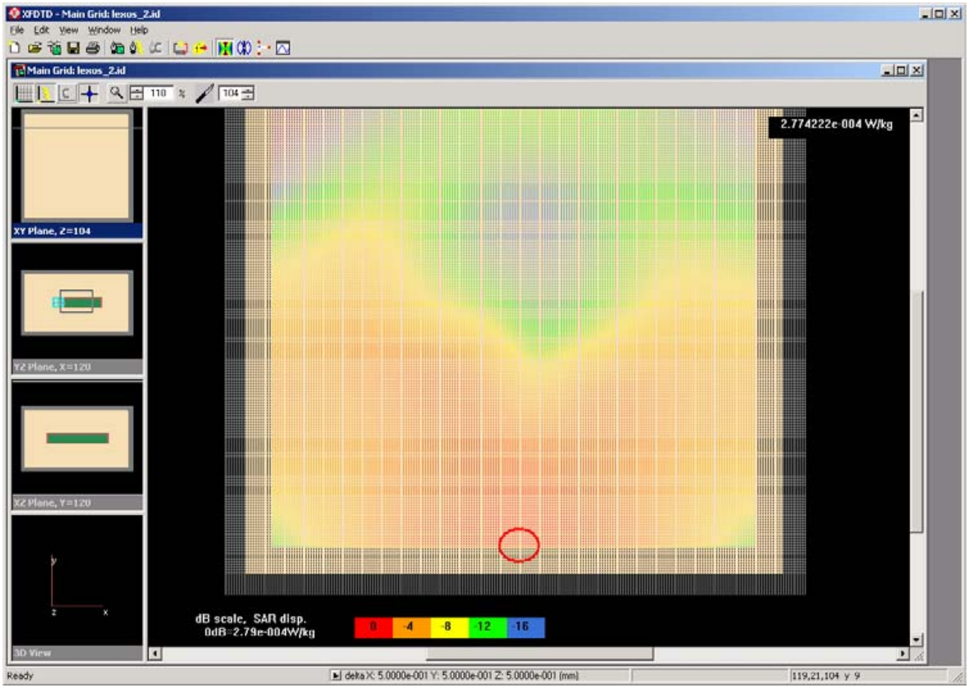

Figure 14 1 gram SAR average 10 mm above Lexos. A maximum SAR of 277 μW/kg is indicated.

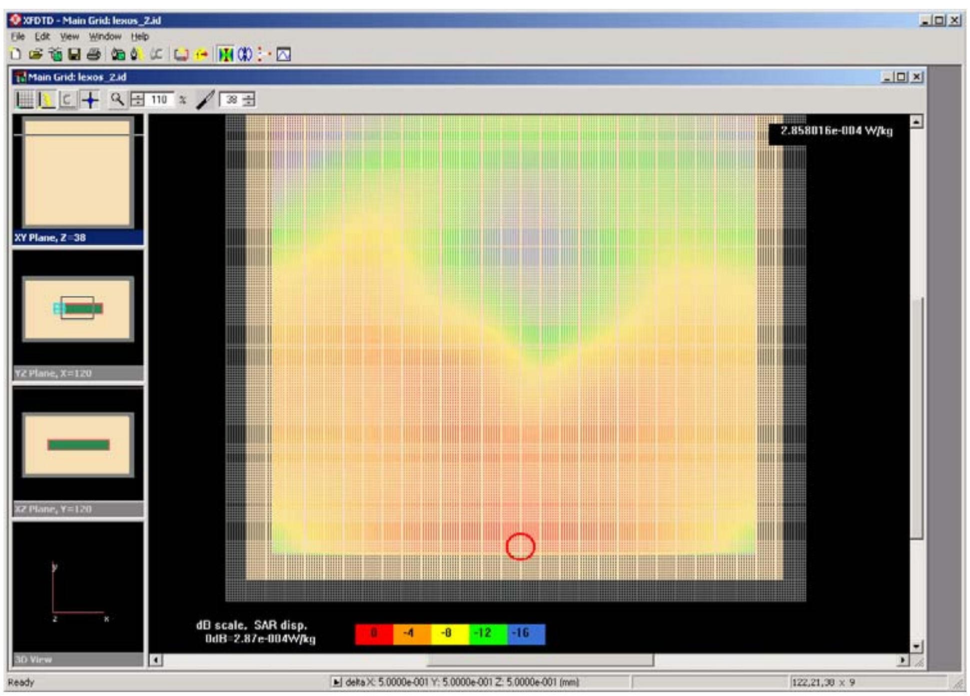

Figure 15 1 gram SAR average 10 mm below Lexos. A maximum SAR of 285 μW/kg is indicated.

In these latter 4 figures, the 1 gram average SAR is <800 μW/kg. The location of the maximum 1 gram average SAR of 793 μW/kg is found to exist very close to the antenna.

Device orientation relative to modeled body.

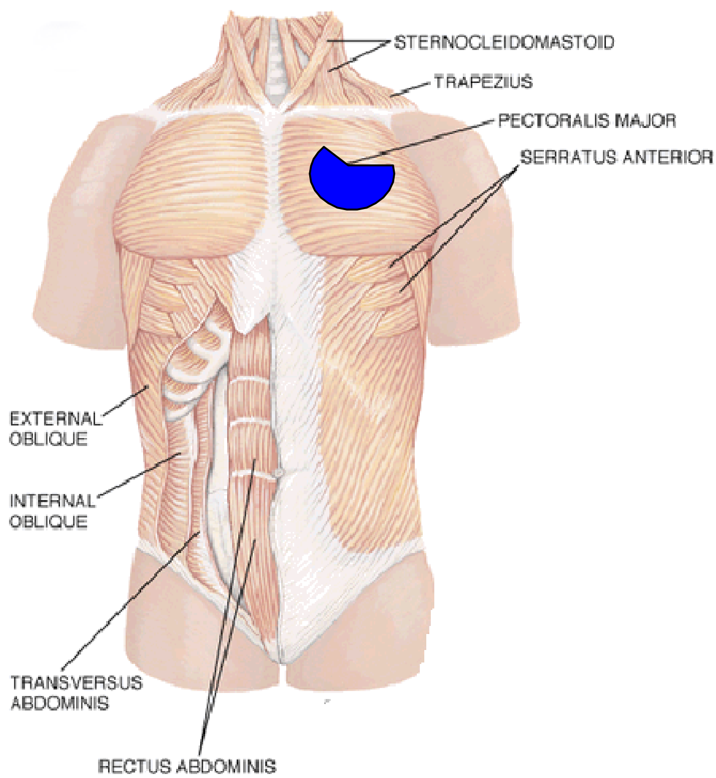

Figure 16 Location of Lexos ICD relative to upper torso

Figure 16 shows the typical location of an ICD implant relative to a human torso. The implant is placed in a small distance below the subcutaneous tissue, often residing within the muscular tissue as well. The implant can be placed in the right or left side of the torso.